Jurnal Kejuruteraan 32(4) 2020: 735-742
https://doi.org/10.17576/jkukm-2020-32(4)-25

Characterization of Titanium Alloy-Hydroxyapatite Composite through Powder Injection Molding

Mohd Ikram Ramli[a], Farhana Mohd Foudzi[b]*, Abu Bakar Sulong[b], Fatin Aqilah Abdul Yazid[b], Norhamidi Muhamad[b], David Hui[c]

[a]*Department of Mechanical Engineering, Faculty of Engineering, City University Malaysia, Menara City U, No. 8, Jalan 51A/223,46100, Petaling Jaya, Selangor Darul Ehsan, Malaysia*
[b]*Department of Mechanical Engineering and Manufacturing, Faculty of Engineering and Built Environment, Universiti Kebangsaan Malaysia, 43600 Bangi Selangor, Malaysia*
[c]*Department of Mechanical Engineering, University of New Orleans, Engineering Building, EN 909, 2000 Lakeshore Drive, New Orleans, LA 70148*

**Corresponding author: farhana.foudzi@ukm.edu.my*

Received 4 February 2020, Received in revised form 30 June 2020
Accepted 1 July 2020, Available online 30 November 2020

ABSTRACT

Powder injection moulding (PIM) is a process that combines the technologies of plastic injection moulding and powder metallurgy. The fabrication of titanium alloy-hydroxyapatite (Ti6Al4V/HA) composite using PIM is still poorly reported due to the difficulties in processing two different materials namely the metal and ceramic. Such promising composite can be proposed as an implant material due to its great properties. Hence, this work aims to characterise the properties of Ti6Al4V/HA composite produced by PIM. In this work, 90 wt% of Ti6Al4V and 10 wt% of HA were mixed with a binder system of 60 wt% palm stearin and 40 wt% polyethylene. The powder loading of the feedstock was 66 vol%. The feedstock with a pseudoplastic flow is preferred in PIM as fewer defects are formed during the injection moulding process. Moreover, the binders are removed in two stages namely the solvent and thermal debinding. Based on the observation, the removal of palm stearin created capillary routes that help to remove polyethylene during thermal debinding. Next, sintering was performed at three different temperatures, which include 1100°C, 1200°C and 1300°C. The heating rate, holding time and cooling rate was set at 3°C/min, 90 min and 6°C/min, respectively. It was found that Ti6Al4V/HA sintered at 1300°C yielded the highest density of 4.13 g/cm^3. In addition, such sintered part also generated the highest flexural and Young's modulus with the values of 86.4 MPa and 15.04 GPa, respectively. These values are approximately in the range of the physical and mechanical properties of the extant bone-implant.

Keywords: Powder injection molding; Ti6Al4V/HA composite, Rheological properties, Physical and mechanical properties

INTRODUCTION

Powder injection moulding (PIM) is a manufacturing process that fabricates desired parts made of metals or ceramics. It uses the fundamentals of plastic injection moulding and powder metallurgy (German & Bose 1997) to enhance the properties of these technologies to produce high precision shapes (Raza et al. 2014). Having said that, PIM is widely employed in various industries due to its capability is producing near net shape products. Such near shape products with complex geometries and high dimensional accuracy are achievable without the incorporation of secondary processes such as machining (Chakartnarodom et al. 2016). Moreover, PIM is also capable in mass production of desired products at a competitive cost. PIM is more capable to produce parts with greater mechanical properties and better surface finish compared to other powder metallurgy methods such as heat suppression moulding (Hayat et al. 2017). Generally, PIM involved four main stages (Thian et al. 2011) namely mixing, injection moulding, debinding and sintering (Heng et al. 2013). In the first step, metal or ceramic powders are mixed with binders to produce a feedstock (Emeka et al. 2017). Binders are added to hold the metal or ceramic particles so the particles could flow through the injection moulding process smoothly. Binders also provide adequate strength for handling purposes, so that the injected part will not fracture prior to sintering process (Atre et al. 2003). Following the mixing process, the feedstock will be injected into a mould. The injected part is commonly known as the green part. Then, the binders will be removed from the green part to produce the brown part (Foudzi et al. 2013). Finally, the brown part will be sintered to produce the desired

final part with great physical and mechanical properties.

PIM has been recently incorporated in the biomedical field and has been claimed to be one of the preferred methods in producing implants for orthopaedic and dental (Hamidi et al. 2017). Titanium alloy (Ti6Al4V) is widely used in such applications due to its mechanical properties, biocompatibility and resistance to corrosion (Raza et al. 2014). Moreover, Ti6Al4V is also incorporated in medical devices as a replacement for hard tissues like dental implants, bone plates and hip joints (Li & Kawashita 2011). It also has a high degree of chemical resistance and good biocompatible properties (Sidambe et al. 2012). Despite these beneficial properties, Ti6Al4V is not a good stand-alone implant material. It is because its Young's modulus is higher than that of human bones which resulted in stress shielding (Salleh et al. 2017). Having said that, hydroxyapatite (HA) or $(Ca_{10}(PO_4)_6(OH)_2)$, is a calcium phosphate ceramic commonly used in the biomedical field. It is a natural organic component of living tissues commonly used in medical implants due to its bioactive properties which are capable of stimulating bone growth (Miranda et al. 2016). Hence, HA which is a bioceramic material is known for its similarities in chemical composition and biological properties with those of human bones (Dantas et al. 2017). However, tensile strength for HA is poor compared to human bones, therefore, it is not suitable for medical implants with high loading applications because it can easily crack (Hamidi et al. 2017). To prevent cracks, the addition of biometal elements to HA have been investigated. According to (Niespodziana et al. 2010), the combination of Ti6Al4V and HA seemed promising as an alternative implant material. A similar approach was also employed (Eriksson et al. 2006) using the compaction process, whereby, high density sintered Ti6Al4V/HA parts were achieved. A porous Ti6Al4V/HA composite was also successfully produced using a space holder through PIM (Raza et al. 2015). The compressive strength for such a porous composite is 370 MPa. In this research, the Ti6Al4V/HA composite was produced using the PIM method. The objective of this work is to study the effect of different sintering temperatures on the density and strength of sintered Ti6Al4V/HA composite. This composite is expected to be biocompatible with good biological, physical and mechanical properties suitable for medical implants.

METHODOLOGY

Figure 1 indicates the particles of (a) Ti6Al4V and (b) HA powders. The average particle size for both materials was measured using a Malvern Particle Size Analyzer. The average particle size for Ti6Al4V and HA is 20 µm and 5µm, respectively. The particle size was obtained using the D_{50} distribution (Arifin 2015). Before preparing the feedstock, critical powder loading for Ti6Al4V/HA was determined using the critical powder volume percentage (CPVP) test based on ASTM D-281-31. This test is carried out using oleic acid to determine the suitable powder loading. Based on the CPVP test (Figure 2), the suitable powder loading was estimated at 66 vol%. This value is deemed adequate for powder loading because the volume of powder is more than 50 %. If the volume of powder is more than that of the binder, defects during debinding and sintering processes such as breakage and contraction of parts can be prevented (German & Bose 1997). Hence, based on the suitable powder loading of 66 vol%, the feedstock was produced by mixing 90 wt% of Ti6Al4V and 10 wt% of HA (90:10), with a binder system of 60 wt% palm stearin (PS) and 40 wt% polyethylene (PE). The mixing process employed the Brabender mixer where the mixing temperature and speed were kept constant at 150 ^{o}C and 25 rpm, respectively (Foudzi et al. 2013).

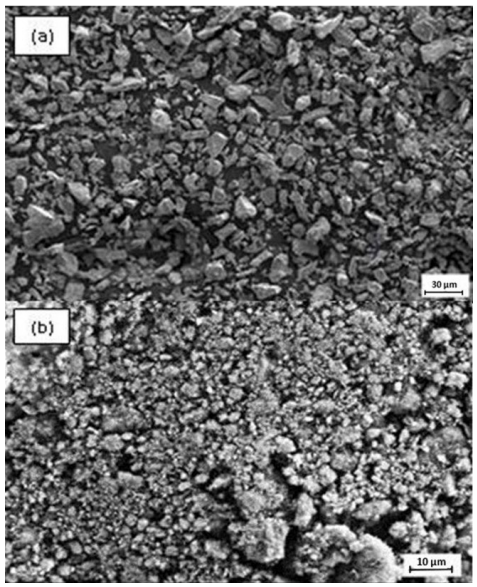

FIGURE 1. SEM images of (a) Ti6Al4V and (b) HA powder particles

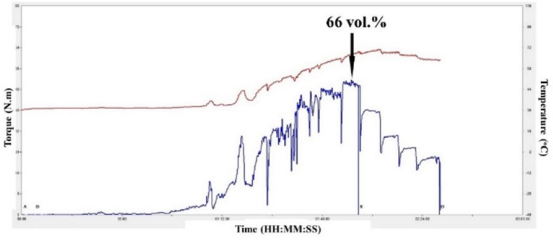

FIGURE 2. Graph of CPVP test for 90:10 (Ti6Al4V/HA) powder

The main purpose of the rheology test is to evaluate the flow type of the feedstock whether it is pseudoplastic, dilatant or Newtonian. According to available reports, the most preferred flow type in PIM is pseudoplastic (German & Bose 1997). The rheological properties of 66 vol% feedstock were investigated using a capillary rheometer machine (Shimadzu CFT-500D) with a capillary diameter of 1 mm. The rheology test was carried out at three different temperatures, 150 ºC, 160 ºC and 170 ºC, using different loads (320 N, 340 N, 360 N and 380 N). The next stage is injection moulding where it is performed using a semi-automatic table-top injection moulding machine (DSM Xplore injection moulding machine 10CC). The injection parameters such as injection temperature, mould temperature and injection pressure were set at 160 ºC, 100 ºC and 8 bar, respectively (Arifin 2015). These values are expected to not form any defects on the injected part. The third process which is debinding, is carried out in two stages involving solvent and thermal debinding. Debinding is performed to remove the binders prior sintering. During solvent debinding, the strength of the injected part (green part) can be maintained although the debinding time may be short. At this stage, the injected Ti6Al4V/HA composite is immersed in a heptane solution at the temperature of 60 ºC for 60 min to remove PS. The second stage of debinding, thermal debinding, is carried out at two different temperatures namely 320 ºC to remove PS and 500 ºC to remove PE (Arifin 2015). The dwell time for both stages is 60 min. It is important to note that the removal of PS is carried out twice in both stages of debinding. During solvent debinding, the removal of PS will form capillary routes that will ease the removal of PE during thermal debinding. However, PS is not completely removed during solvent debinding. It is once again removed at a higher temperature (320 ºC) during thermal debinding. A small fraction of binders are still needed to hold the powder particles before sintering. Once the binders are removed, the green part becomes the brown part. The final stage of sintering is performed on the brown part using a vacuum furnace (Korea VAC-TEC VTC 500HTSF) at different temperatures of 1100 ºC, 1200 ºC and 1300 ºC. The holding time is 90 min (Arifin 2015). The heating and cooling rates are 3 ºC/min and 6 ºC/min, respectively (Salman et al. 2009). The sintered part were tested for its physical and mechanical properties such as density, flexural strength and Young's modulus. The density of the sintered part is measured based on Metal Powder Industries Federation (MPIF) Standard 42 that uses the Archimedes method. The mass of the sintered part will be measured twice, before and after immersing in water using an electronic mass balance of Sartorius model BSA224S-CW. Meanwhile, flexural strength is measured based on a three-point bending test using the Universal Testing Machine INSTRON 5567. The test is based on the MPIF Standard 15. In order to obtain the flexural strength, the Transverse Rupture Strength (TRS) formula is used where TRS and F are denoted by flexural strength and load, respectively. While L, h and b are the lengths, height and width of the sample, respectively.

$$TRS = \frac{3FL}{2h^2b} \quad (1)$$

Apart from the physical and mechanical properties, the morphological assessment was also conducted on the green, brown and sintered parts. For the microstructure analysis, the sintered Ti6Al4V/HA parts were grounded and polished before observation using a Mitutoyo optical microscope. Meanwhile, for the morphological analysis, Hitachi S-3400N scanning electron microscopy (SEM) was used. The magnification for the morphology observation was set at 500x and 1500x.

RESULTS AND DISCUSSION

FEEDSTOCK PREPARATION

Figure 3 illustrates the relationship between torque and time during the mixing process. During the initial period of mixing, the values of torque increased significantly. The increase is due to the addition of binders into Ti6Al4V/HA powder. The mixing temperature was set at 150 ºC, exceeding the highest melting temperature of the binders. Such a temperature allows the portioning of powder particles to occur due to the high viscosity of the binders (Supati et al. 2000). Meanwhile, the increasing temperature during mixing is due to the friction that occurs between the powder particles and also the friction between the powder particles and the surface of the mixer blade of the mixing machine. Therefore, these frictions produce heat (temperature increases). Based on Figure 3, the torque decreased and became stagnant at 20 N.m during the final stage of the mixing process. At this stage, it can be concluded that the binders have filled the empty spaces between the powder particles. In addition, the binders have moistened the feedstock resulting in the decrement of the viscosity of feedstock. Therefore, at this stage, the feedstock is said to be homogeneously mixed. Moreover, it has also been reported that the uniform value of torque during mixing indicates that the feedstock has reached its homogeneity (Liu et al. 2005).

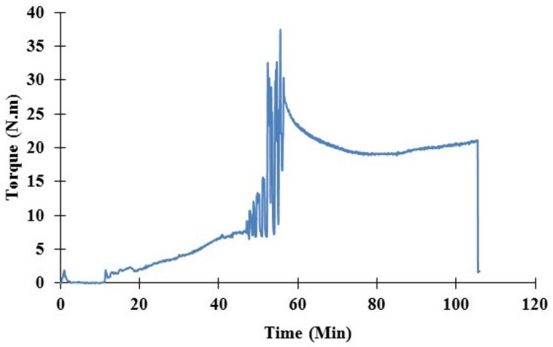

FIGURE 3. Torque behavior of feedstock during mixing process

RHEOLOGICAL BEHAVIOR

Rheological tests were conducted at three different temperatures, 150 °C, 160 °C and 170 °C. These temperatures were selected based on the highest melting point of PE and the lowest melting point of PS. Figure 4 indicates the rheological result where the viscosity decreased with the increasing shear rate at all temperatures. (German & Bose 1997) have theoretically mentioned that the viscosity of the feedstock in the PIM process should be within the range of 10 Pa.s to 1000 Pa.s at all temperatures tested. Meanwhile, the range of shear rate was 10^2 s^{-1} to 10^5 s^{-1}. Based on this theory, it can be concluded that for the 66 vol% powder loading of Ti6Al4V/HA, the viscosity and shear rate were within the preferred range. These values confirmed that the flow behaviour type as depicted in Figure 4 was pseudoplastic. It is due to the reduction in the friction force between the binders and also the friction between the powder particles and the binders. Feedstock with pseudoplastic flow requires little energy during the injection moulding process to form a complex geometry of parts (Ahn et al. 2009). Also, this flow type is preferred in PIM due to its capability to produce a green part that is free from defects. Furthermore, the relationship between the viscosity and shear rate can also be explained through the flow behaviour index, n, which determines whether the flow type of feedstock is pseudoplastic, Newtonian or dilatant. n is calculated using the Power Law where η, K, γ and n denote the viscosity (Pa.s), constant, shear rate and flow index, respectively. Whereby, values of η and γ can be obtained directly from the rheology graphs.

$$Power\ Law;\ \eta = K\gamma^{(n-1)} \quad (2)$$

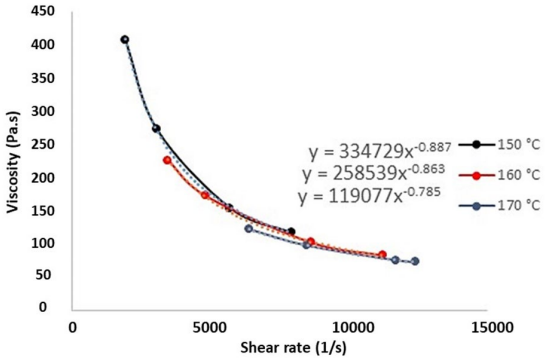

FIGURE 4. Pseudoplastic behavior for feedstock at all temperature

Table 1 demonstrates the flow behaviour index (n) from the 66 vol% powder loading of Ti6Al4V/HA at all temperatures, 150 °C, 160 °C and 170 °C. The n for all Ti6Al4V/HA feedstocks was less than 1, indicating pseudoplastic flow type and is suitable for injection (Karatas et al. 2004).

TABLE 1. Flow index (n) of Ti6Al4V/HA feedstock

Temperature (°C)	Flow behavior index, n
150	0.113
160	0.137
170	0.215

INJECTION MOLDING PROCESS

The green part was successfully injected using the mentioned parameters. Figure 5 illustrates the injected green part with no obvious defects observed on the surface such as short shot and splashing. The morphological studies on the injected Ti6Al4V/HA green part were performed using the SEM at 500x and 1000x magnification scales (Figure 6). Based on the observation, Ti6Al4V and HA particles (lighter region) were well coated with the PS and PE binders (darker region). However, it is difficult to distinguish the Ti6Al4V and HA particles due to the same colour region. Therefore, HA is represented by the smaller particles due to its smaller size of 5 µm compared to Ti6Al4V.

FIGURE 5. Injected green part

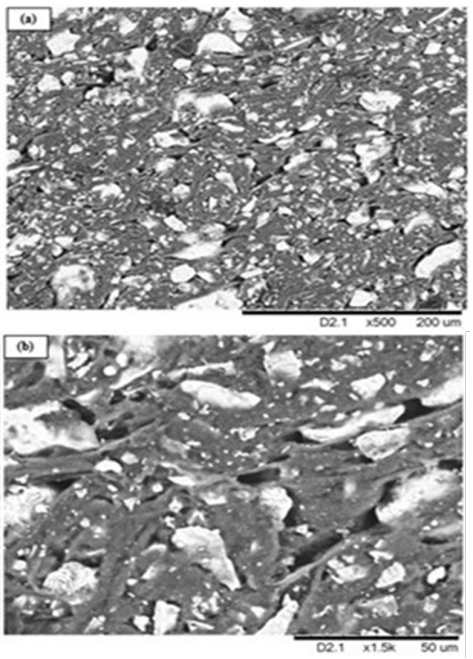

FIGURE 6. SEM images of the injected Ti6Al4V/HA green part at (a) 500x and (b) 1500x magnification

DEBINDING PROCESS

The PS and PE binders were removed by solvent and thermal debinding processes. Following the completion of the debinding process, the green part is known as a debound brown part (Figure 7). It was observed that the color of debound part is different from green part (Figure 5) which is lighter. Using the same scale of magnifications, Figure 8 illustrates the SEM images of Ti6Al4V/HA brown part. Based on the observation, the Ti6Al4V and HA particles were more exposed due to the removal of binders. It is also observed that pores or capillary routes were formed in the debound brown part (Figure 8(a)) compared to the green part (Figure 6(a)). However, the binders (darker region) were still present in the brown part. It was observed that Ti6Al4V and HA particles (lighter region) were still coated with the PS and PE binders (Figure 8). The purpose of the remaining binders in the brown part is to provide enough strength before sintering. It is because the brown part is fragile, hence, needs adequate strength for handling purposes.

FIGURE 7. Debound brown part

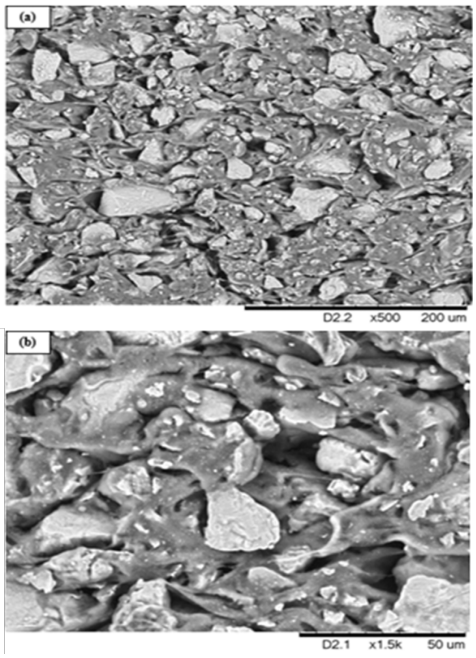

FIGURE 8. SEM images of the debound brown part at (a) 500x and (b) 1500x magnification

SINTERING PROCESS

The sintering process was conducted on the brown part of Ti6Al4V/HA at three different temperatures, 1100 ºC, 1200 ºC and 1300 ºC. It is quite a challenging process because the high temperatures of Ti6Al4V can lead to the decomposition of HA (Raza et al. 2014). Figure 9 represents the sintered Ti6Al4V/HA parts at all sintering temperatures. For the sintered Ti6Al4V/HA at 1300 °C, a minor swelling was observed. The swelling occurred due to the remaining binders that were not eliminated during the debinding process (German & Bose 1997). It can also be observed that the sintered part is brightest in colour compared to the green and brown parts. The differences in colour for the green, brown and sintered parts are illustrated in Figure 10.

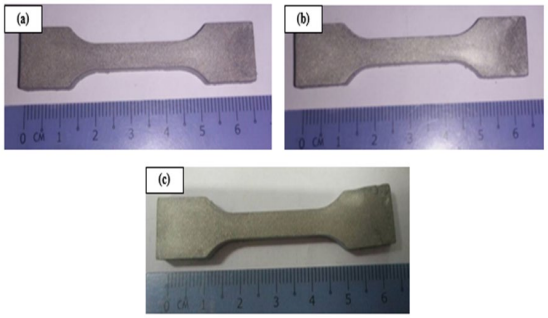

FIGURE 9. Sintered parts after sintering process at (a) 1100 ºC, (b) 1200 ºC and (c) 1300 ºC

FIGURE 10. Comparison of (a) injected green part, (b) debound brown part and (c) sintered part at 1300 ºC

Figure 11 indicates the SEM images of the sintered Ti6Al4V/HA parts at all sintering temperatures. Lower sintering temperature (1100 ºC) formed a significant porous region compared to higher sintering temperature (1300 ºC). Moreover, Ti6Al4V was not fully sintered at the sintering temperatures of 1100 ºC and 1200 ºC, as depicted in Figures 11 (a) and (b), respectively. However, at the sintering temperature of 1300 ºC, necking formation occurred and clear grain boundaries were observed due to the reduction of the pore region. Therefore, it can be concluded that the Ti6Al4V brown part is successfully sintered at a sintering temperature of 1300 ºC.

PHYSICAL AND MECHANICAL PROPERTIES OF SINTERED PART

Figure 12 indicates the density of the Ti6Al4V sintered parts at all sintering temperatures. Based on the values, the density increased with increasing sintering temperature. The highest density was gained when Ti6Al4V was sintered at 1300 ºC (4.13 g/cm^3). The value accounted for 98% of the theoretical value which is 4.18 g/cm^3. Such high value is achievable due to sufficient diffusion that occurred from the necking process between the particles resulting in less pore region. Therefore, it is confirmed that the sintering temperature of 1300 ºC is the best compared to 1100 ºC and 1200 ºC to achieve a fully dense final sintered part.

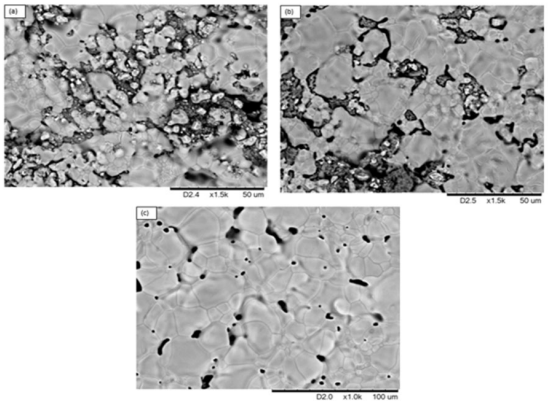

FIGURE 11. SEM images of Ti6Al4V/HA sintered part at sintering temperatures of (a) 1100 ºC, (b) 1200 ºC and (c) 1300 ºC

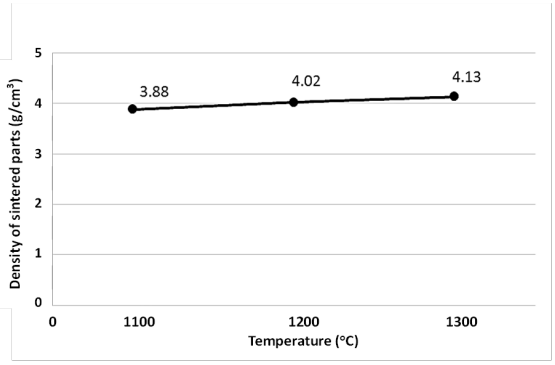

FIGURE 12. Density of sintered part at sintering temperatures of (a) 1100 ºC, (b) 1200 ºC and (c) 1300 ºC

Based on Figure 13, the same trend from the density test was observed for the flexural strength where the lowest and highest values of flexural strength were produced by the sintered Ti6Al4V/HA at 1100 ºC and 1300 ºC, respectively. The significant increment of flexural strength from the sintering temperature of 1200 ºC to 1300 ºC is due to the grain boundaries formed from adequate diffusion. Also, the flexural strength measured at 1300 ºC sintering temperature was within the range of human bone strength, 60 – 130 MPa (Hamidi et al. 2017; Han et al. 2017).

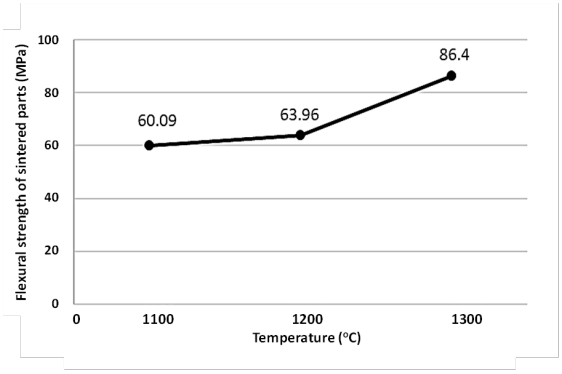

FIGURE 13. Flexural strength of sintered part at sintering temperatures of (a) 1100 °C, (b) 1200 °C and (c) 1300 °C

Figure 14 denotes the values of Young's modulus which gradually increased with the increasing sintering temperatures. The increasing density resulted in denser and higher strength sintered part (Cihlář & Trunec 1996). Young's modulus is calculated from the gradient of the elastic region of the stress-strain graph. The graph was obtained from the flexural strength test (three-point bending). Using the graph, Young's modulus can be easily calculated from the gradient of the elastic region prior to reaching the yield point. Based on Figure 14, the values for sintered Ti6Al4V/HA at 1200 °C and 1300 °C were in the range of Young's modulus for human bones (10 GPa – 30 GPa) (Arifin et al. 2014).

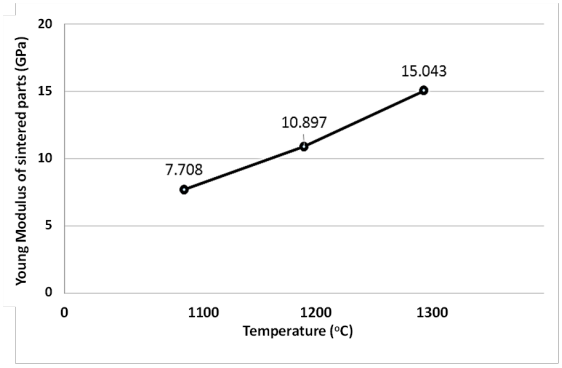

FIGURE 14. Young's Modulus of sintered part at sintering temperatures of (a) 1100 °C, (b) 1200 °C and (c) 1300 °C

CONCLUSION

The fabrication of Ti6Al4V/HA composite through the PIM process was successfully conducted. The flow type of the Ti6Al4V/HA feedstock was determined as pseudoplastic which is suitable for the injection moulding process where no defects were observed. The debinding process that eliminated the PS and PE binders was carried out in two stages namely solvent and thermal debinding. The removal of PS created capillary routes to help in the removal of PE during the thermal debinding stage. However, binders were not completely removed prior to sintering. The remaining binders helped to provide adequate strength to the fragile debound parts. On the other hand, sintering was conducted at three different temperatures (1100 °C, 1200 °C and 1300 °C). Based on the evaluation of physical and mechanical properties, it can be concluded that Ti6Al4V/HA sintered at 1300 °C produced the best properties in terms of density, flexural strength and Young's modulus. The values for all these properties were found to be in the range of that of the human bone. Therefore, Ti6Al4V/HA composite seems promising to be further explored as an alternative implant material due to its great mechanical properties.

ACKNOWLEDGEMENT

This work was supported by Grant No. DCP-2017-001/2 and FRGS/1/2017/TK03/UKM/02/1 from the Malaysian Ministry of Education (MOE).

DECLARATION OF COMPETING INTEREST

None.

REFERENCES

Ahn, S., Park, S.J., Lee, S., Atre, S.V. & German, R. M. 2009. Effect of powders and binders on material properties and molding parameters in iron and stainless steel powder injection molding process. *Powder Technology* 193(2): 162–169.

Arifin A., Sulong A.B., Muhamad N., Syarif J. & Ramli M.I. 2014. Materials processing of hydroxyapatite and titanium alloy (HA/Ti) composite as implant materials using powder metallurgy: A review. *Materials & Design* 55: 165-175.

Arifin, A., 2015. Powder injection moulding of hydroxyapatite/titanium alloy (Ti6Al4V) composite, Doctoral Thesis, Universiti Kebangsaan Malaysia.

Atre, S.V., German, R.M. & De Souza, J.P. 2003. Effect of mixing on the rheology and particle characteristics of tungsten-based powder injection molding feedstock. *Materials Science and Engineering: A* 356(1-2): 337–344.

Chakartnarodom, P., Kongkajun, N. & Chuankrerkkul, N. 2016. Powder injection molding of mullite: the study of binder dissolution behavior during debinding step using statistical methods. *Key Engineering Materials* 690: 87–91.

Cihlář, J. & Trunec, M. 1996. Injection moulded hydroxyapatite ceramics. *Biomaterials* 17(19): 1905–1911.

Dantas, T.A., Abreu, C.S., Costa, M.M., Miranda, G., Silva, F.S., Dourado, N. & Gomes, J.R. 2017. Bioactive materials driven primary stability on titanium biocomposites. *Materials Science and Engineering: C* 77: 1104–1110.

Emeka, U.B., Sulong, A.B., Muhamad, N., Sajuri, Z. & Salleh, F.M. 2017. Two component injection molding of bi-material of stainless steel and yttria stabilized zirconia-green part. *Jurnal Kejuruteraan* 29(1): 49–55.

Eriksson, M., Andersson, M., Adolfsson, E., & Carlström, E. 2006. Titanium–hydroxyapatite composite biomaterial for dental implants. *Powder metallurgy* 49(1): 70-77.

Foudzi, F.M., Muhamad, N., Sulong, A.B. & Zakaria, H. 2013. Yttria stabilized zirconia formed by micro ceramic injection molding; rheological properties and debinding effects on the sintered part. *Ceramics International* 39: 2665–2674.

German, R.M. & Bose, A. 1997. Injection Molding of Metals and Ceramics. 1st edition, Metal Powder Industries Federation, Princeton, New Jersey.

Hamidi, M.F.F.A., Harun, W.S.W., Samykano, M., Ghani, S.A.C., Ghazalli, Z., Ahmad, F. & Sulong, A.B. 2017. A review of biocompatible metal injection molding process parameters for biomedical applications. *Materials Science and Engineering: C* 78: 1263–1276.

Han, C., Wang, Q., Song, B., Li, W., Wei, Q., Wen, S., Liu, J. & Shi, Y. 2017. Microstructure and property evolutions of titanium/nano-hydroxyapatite composites in-situ prepared by selective laser melting. *Journal of the Mechanical Behavior of Biomedical Materials* 71: 85–94.

Hayat, M.D., Goswami, A., Matthews, S., Li, T., Yuan, X. & Cao, P. 2017. Modification of PEG/PMMA binder by PVP for titanium metal injection molding. *Powder Technology* 315: 243–249.

Heng, S.Y., Muhamad, N., Sulong, A.B., Fayyaz, A. & Amin, S.Y.M. 2013. Effect of sintering temperature on the mechanical and physical properties of WC-10% Co through micro-powder injection molding µPIM. *Ceramics International* 39: 4457–4464.

Karatas, C., Kocernal, H.I., Saritas, S. 2004. Rheological properties of feedstocks prepared with steatite powder and polyethylene-based thermoplastic binders. *Journal of Materials Processing Technology* 152(1): 77–83.

Li, Z. & Kawashita, M. 2011. Current progress in inorganic artificial biomaterials. *Journal of Artificial Organs* 14(3): 163–170.

Liu, L., Loh, N.H., Tay, B.Y., Tor, S.B., Murakoshi, Y. & Maeda, R. 2005. Mixing and characterization of 316L stainless steel feedstock for micro powder injection molding. *Materials Characterization* 54(3): 230–238.

Miranda, G., Araújo, A., Bartolomeu, F., Buciumeanu, M., Carvalho, O., Souza, J.C.M., Silva, F.S. & Henriques, B. 2016. Design of Ti6Al4V-HA composites produced by hot pressing for biomedical applications. *Materials and Design* 108: 488–493.

Niespodziana, K., Jurczyk, K., Jakubowicz, K. & Jurczyk, M. 2010. Fabrication and properties of titanium-hydroxyapatite nanocomposites. *Materials Chemistry and Physics* 123(1): 160–165.

Raza, M.R., Ahmad, F., Muhamad, N., Sulong, A.B., Omar, M.A., Akhtar, M.N., Nazir, M.S., Muhsan, A.S. & Aslam, M. 2014. Effects of residual carbon on microstructure and surface roughness of PIM 316L stainless steel. *Proceedings of International Civil and Infrastructure Engineering Conference (InCIEC)* 927 – 935.

Raza, M.R., Sulong, A.B., Muhamad, N., Akhtar, M.N., & Rajabi, J. 2015. Effects of binder system and processing parameters on formability of porous Ti/HA composite through powder injection molding. *Materials & Design* 87: 386-392.

Salleh, F.M., Sulong, A.B., Muhamad, N., Mohamed, I. F., Mas'ood, N.N. & Ukuweze, B.E. 2017. Co-powder injection molding (co-PIM) processing of titanium alloy (Ti6Al4V) and hydroxyapatite (HA). *Procedia Engineering* 184: 334–343.

Salman, S., Gunduz, O., Yilmaz, S., Öveçoğlu, M.L., Snyder, R.L., Agathopoulos, S. & Oktar, F.N. 2009. Sintering effect on mechanical properties of composites of natural hydroxyapatites and titanium. *Ceramics International* 35(7): 2965-2971.

Sidambe, A.T., Dergutti, F. & Todd, I. 2012. Metal injection molding of low interstitial titanium. *Key Engineering Materials* 520: 145–152.

Standard M.P.I.F. 2006. Method for determination of transverse rupture strength of powder metallurgy materials. MPIF Standard Test Methods 4.

Supati, R., Loh, N.H., Khor, K.A. & Tor, S.B. 2000. Mixing and characterization of feedstock for powder injection molding. *Materials Letters* 46(2-3): 109–114.

Thian, E.S., Loh, N.H., Khor, K.A. & Tor, S.B. 2011. Effects of debinding parameters on powder injection molded Ti-6Al-4V/HA composite parts. *Advanced Powder Technology* 12(3): 361–370.